Electronic Supplementary Information: Ultrafast Channel I and Channel II Charge Generation Processes at a Nonfullerene Donor-Acceptor PTB7:PDI Interface is Crucial for Its Excellent Photovoltaic Performance

Kai Li, Dong-Hui Xu, Xin Wang, and Xiang-Yang Liu*

College of Chemistry and Material Science, Sichuan Normal University, Chengdu 610068, China

E-mail: xiangyangliu@sicnu.edu.cn

Methods

Semi-Classical Spectra Simulation

Absorption spectra are simulated with a semi-classical method proposed by Barbatti et al.[1,2] On the basis of ground-state ensembles composed of N structures $\mathbf{R}_k$, we can calculate photoabsorption cross section with time-dependent perturbation theory at the first-order level

$$\sigma(E) = \frac{\pi e^2}{2mc\varepsilon_0} \sum_{l \neq i} \left[\frac{1}{N} \sum_{k}^{N} f_{il}(\mathbf{R}_k)\, g(E - \Delta E_{il}(\mathbf{R}_k), \delta) \right] \tag{1}$$

where ε_0 is vacuum dielectric constant; c is speed of light; e and m are electron charge and mass; $f_{il}(\mathbf{R}_k)$ and $\Delta E_{il}(\mathbf{R}_k)$ are oscillator strength and transition energy from initial i to final l state at structure $\mathbf{R}_k$; $g(E - \Delta E_{il}(\mathbf{R}_k), \delta)$ is a normalized line shape function that is peaked at transition

energy $\Delta E_{il}(\mathbf{R}_k)$ and broadened by a phenomenological constant δ. In practical applications, there are two kinds of shape functions used to model line shapes. The first one is Gaussian shape function

$$g_{Gauss}(E-\Delta E_{il},\delta) = \left(\frac{2}{\pi}\right)^{1/2} \frac{\hbar}{\delta} exp\left(\frac{-2\left(E-\Delta E_{il}\right)^2}{\delta^2}\right) \tag{2}$$

the second one is Lorentzian shape function

$$g_{Lorentz}(E-\Delta E_{il},\delta) = \frac{\hbar\delta}{2\pi}\left[\left(E-\Delta E_{il}\right)^2 + \left(\frac{\delta}{2}\right)^2\right]^{-1} \tag{3}$$

in which $\hbar$ is reduced Planck constant. Our group has recently implemented this method for absorption spectra simulations.[3–6] In the present work, Gaussian shape function is used for simulating absorption spectra from ground to excited state ($i = 0$).

Fewest-Switches Surface-Hopping Method

Trajectory-based fewest-switches surface-hopping dynamics simulation approaches by Tully et al.[7,8] has been extensively employed to simulate a series of ultrafast excited-state relaxation processes in chemical and biological systems, and materials.[9–24] In the following, a brief presentation is given.

Time-dependent Schrödinger equation can be written as

$$i\hbar\dot{\Psi}(\mathbf{r},\mathbf{R}(t),t) = \hat{H}_0(\mathbf{r},\mathbf{R}(t))\Psi(\mathbf{r},\mathbf{R}(t),t) \tag{4}$$

where $\hat{H}_0(\mathbf{r},\mathbf{R}(t))$ is zero-order electronic Hamiltonian while $\mathbf{r}$ and $\mathbf{R}$ are spatial coordinates of electron and nuclear respectively. Time-dependent electronic wavefunction is then expressed in terms of linear combination of adiabatic zero-order electronic spatial wavefunctions:

$$\Psi(\mathbf{r},\mathbf{R}(t),t) = \sum_{i=1}^{N} C_i(t)\Psi_i(\mathbf{r},\mathbf{R}(t)) \tag{5}$$

in which $\Psi_i(\mathbf{r},\mathbf{R}(t))$ is an eigenfunction of zero-order Hamiltonian $\hat{H}_0(\mathbf{r},\mathbf{R}(t))$ at nuclear coordinates $\mathbf{R}(t)$. After inserting Eq. 5 into Eq. 4, multiplying by $< \Psi_j(\mathbf{r},\mathbf{R}(t))|$ from left-hand side, and

integrating over electronic spatial coordinates, we obtain

$$\dot{C}_j(t) = -i\hbar^{-1}C_j(t)E_j(\mathbf{R}(t)) - \sum_i^N C_i(t)\tau_{ji}(t) \tag{6}$$

where $\tau_{ji}(t) =< \Psi_j \mid \frac{\partial}{\partial t} \mid \Psi_i >$ is time derivative nonadiabaic coupling between different adiabatic states. $\tau_{ji}(t)$ can also be expressed as $\mathbf{v}(t) \cdot \mathbf{d}_{ji}(\mathbf{R}(t))$ in which $\mathbf{v}(t)$ and $\mathbf{d}_{ji}(\mathbf{R}(t))$ are nuclear velocities and adiabatic derivative couplings respectively. Therefore, Eq. 6 can also be written as

$$\dot{C}_j(t) = -i\hbar^{-1}C_j(t)E_j^0(\mathbf{R}(t)) - \sum_i^N C_i(t)\mathbf{v}(t) \cdot \mathbf{d}_{ji}(\mathbf{R}(t)) \tag{7}$$

which is the central equation of fewest-switches surface-hopping method and can describe radiationless transitions between electronic states with same spins. Fewest-switches criterion finally yields transition probability from i to j states

$$p_{ij}(t)dt = 2\frac{Re(C_i^* C_j \tau_{ij})}{C_i^* C_i}dt \tag{8}$$

This method has been implemented in GTSH package that is initially developed by Prof. Ganglong Cui and Prof. Walter Thiel[25] and interfaced with TDDFT method by Dr. Xiang-Yang Liu under the supervision of Prof. Ganglong Cui.[3–6,26] The developed methods have been widely used to simulation photoinduced ultrafast processes of various systems in both gas and solution phases.

Time-Derivative Nonadiabatic Couplings

Time derivative nonadiabaic couplings $\tau_{ji}(t)$ can be calculated from adiabatic derivative couplings $\mathbf{d}_{ji}(\mathbf{R}(t))$ and nuclear velocities $\mathbf{v}(t)$ and there are also some analytical algorithms for $\mathbf{d}_{ji}(\mathbf{R}(t))$.[27–29] In addition, there are two types of numerical algorithms available to directly compute $\tau_{ji}(t)$ in the framework of TD-DFT.[30,31] Our present work uses recently developed algorithm that has been demonstrated more efficient than previous algorithm.[3,31] A brief presentation is given below, in which subscripts $a, b, c...$ denote virtual orbitals; $i, j, k...$ label occupied orbitals; and $p, q, r...$ are for any type of orbitals.

In TD-DFT, total electronic wave function of an electronically excited state Ψ_K is approximately

written as linear combination of singly excited Slater determinants,

$$\Psi_K = \sum_{i}^{occ} \sum_{a}^{unocc} w_{ia}^K \psi_i^a \tag{9}$$

in which w_{ia}^K stands for coefficient of excited Slater determinant ψ_i^a. Slater determinant $\psi_i^a = \hat{a}_a^\dagger \hat{a}_i \psi_0$ is constructed through electron creation and annihilation operations on ground-state determinant ψ_0. In this situation, time derivative nonadiabatic coupling term between states K and J, namely $\tau_{KJ} =< \Psi_K \mid \frac{\partial}{\partial t} \mid \Psi_J >$, can be further written as

$$\tau_{KJ} = \sum_{ijab} \left(w_{ia}^K \partial_t w_{jb}^J \left\langle \psi_i^a \middle| \psi_j^b \right\rangle + w_{ia}^K w_{jb}^J \left\langle \psi_i^a \middle| \partial_t \psi_j^b \right\rangle \right) \tag{10}$$

The first term is transformed to $\sum_{ia} w_{ia}^K \partial_t w_{ia}^J$ concerning Slater-Condon rule. Time differentiation on ψ_j^b is

$$\partial_t \psi_j^b = \sum_{k \neq j} \psi_{jk}^{bk'} + \psi_j^{b'} \tag{11}$$

where $\psi_p^{q'}$ means that molecular orbital ϕ_p is replaced with time derivative $\partial_t \phi_q$. Therefore, the second term becomes

$$\left\langle \psi_i^a \middle| \partial_t \psi_j^b \right\rangle = \sum_{k \neq j} \left\langle \psi_i^a \middle| \psi_{jk}^{bk'} \right\rangle + \left\langle \psi_i^a \middle| \psi_j^{b'} \right\rangle \tag{12}$$

in which the last term is reduced to $\delta_{ij} \langle \phi_a | \partial_t \phi_b \rangle$ because only one term with $k = i$ and $a = b$ from sum over k survives due to orthogonality condition $\left\langle \phi_p \middle| \partial_t \phi_p \right\rangle = 0$ for real orbitals and $\left\langle \phi_p \middle| \phi_q \right\rangle = \delta_{pq}$. Then, we arrive at

$$\left\langle \psi_i^a \middle| \partial_t \psi_j^b \right\rangle = \delta_{ij} \langle \phi_a | \partial_t \phi_b \rangle - P_{ij} \delta_{ab} \langle \phi_j | \partial_t \phi_i \rangle \tag{13}$$

where P_{ij} is an additional phase factor that depends on ordering convention for orbitals used in Slater determinants. Finally, computational formula of time derivative nonadiabatic couplings is written as

$$\tau_{KJ} = \sum_{ia} w_{ia}^K \partial_t w_{ia}^J + \sum_{iab} w_{ia}^K w_{ib}^J \langle \phi_a | \partial_t \phi_b \rangle - \sum_{ija} P_{ij} w_{ia}^K w_{ja}^J \langle \phi_j | \partial_t \phi_i \rangle \tag{14}$$

in which those terms related to time differentiation on molecular orbitals can be calculated using finite-

difference scheme

$$\left\langle \phi_p \left| \partial_t \phi_q \right. \right\rangle = \frac{1}{\Delta t} \left\langle \phi_p(t) \left| \phi_q(t+\Delta t) \right. \right\rangle \tag{15}$$

where $\phi_p(t)$ and $\phi_q(t+\Delta t)$ represent molecular orbitals at t and $t+\Delta t$ times, respectively. Detailed derivation of this algorithm can be found in recent literature.[31] The corresponding algorithm has been independently coded into a standalone module in the GTSH package and widely used.[3–6,25]

Fragment-Based Exciton Analysis

There are several different analysis methods capable of examining excited-state characters, intra- and inter-molecular electron and energy transfers of complex systems in particular those donor-acceptor systems. One of the most popular methods is based on analyzing one-electron transition density matrices, which can be implemented in different atomic orbital representations, e.g. nonorthogonal atomic orbitals[32] and orthogonalized Löwdin atomic orbitals.[33] Recently we have implemented a similar analysis method using orthogonalized Löwdin atomic orbital representation.[3–5] In such way, one-electron transition density matrix $\mathbf{T}_{LO}$ is expressed as

$$\mathbf{T}_{\mathrm{LO}} = (\mathbf{S}_{\mathrm{AO}})^{1/2} \mathbf{T}_{\mathrm{AO}} (\mathbf{S}_{\mathrm{AO}})^{1/2} = (\mathbf{S}_{\mathrm{AO}})^{1/2} \left(\mathbf{C}\mathbf{T}_{\mathrm{MO}}\mathbf{C}^{\mathrm{T}}\right) (\mathbf{S}_{\mathrm{AO}})^{1/2} \tag{16}$$

where $\mathbf{C}$ and $\mathbf{S}_{AO}$ are MO coefficients and AO overlap matrices; $\mathbf{T}_{AO}$ and $\mathbf{T}_{MO}$ represent one-electron transition density matrices in AO and MO representations. Due to orthogonalization property of Löwdin atomic orbitals, transition contribution from a to b atoms becomes

$$D_{ab} = \sum_{i \in a, j \in b} (\mathbf{T}_{\mathrm{LO}})^2_{ij} \tag{17}$$

where i and j are indices of atomic orbitals and a and b are indices of atoms. Thus, transition contribution from a fragment D to another fragment A in a system is given by

$$\Omega_{DA} = \sum_{a \in D, b \in A} D_{ab} \tag{18}$$

in which $D = A$ and $D \neq A$ represent local excitation (LE) within D fragment and charge transfer (CT) excitation from D to A fragment. Accordingly, contributions of LE and CT to an interested excited state can be quantitatively obtained.[3–5,32,33] These Ω_{DA} can also be regarded as weights of different fragment-based LE and CT excitons. Moreover, time-dependent electron and hole amounts on a fragment can also be calculated.[5,6] The hole amount on a fragment D, as a result of electron transfer from D to all fragments A, is computed as

$$h_D = \sum_{a \in D} D_{ab} = \sum_{A} \Omega_{DA} \tag{19}$$

while, the electron amount of a fragment A transferred from all fragments D is defined as

$$e_A = \sum_{b \in A} D_{ab} = \sum_{D} \Omega_{DA} \tag{20}$$

Electron-Hole Distance

Electronic excitation always results in many pairs of hole and electron, which are represented as singly excited Slater determinants ψ_i^a in TD-DFT calculations (see above). These electron-hole pairs can be described by occupied and unoccupied MO indices. However, such kind of analysis could be complex if many pairs of MOs are involved. Instead, analyzing spatial distribution of electron and hole produced by all pairs of involved MOs is more useful. In such scheme, hole and electron densities are written as follows[34,35]

$$\rho^{hole}(\mathbf{r}) = \rho_{loc}^{hole}(\mathbf{r}) + \rho_{cross}^{hole}(\mathbf{r}) = \sum_{i \to a} (w_{ia})^2 \phi_i(\mathbf{r}) \phi_i(\mathbf{r}) + \sum_{i \to a} \sum_{j \neq i \to a} w_{ia} w_{ja} \phi_i(\mathbf{r}) \phi_j(\mathbf{r}) \tag{21}$$

$$\rho^{electron}(\mathbf{r}) = \rho_{loc}^{electron}(\mathbf{r}) + \rho_{cross}^{electron}(\mathbf{r}) = \sum_{i \to a} (w_{ia})^2 \phi_a(\mathbf{r}) \phi_a(\mathbf{r}) + \sum_{i \to a} \sum_{i \to b \neq a} w_{ia} w_{ib} \phi_a(\mathbf{r}) \phi_b(\mathbf{r}) \tag{22}$$

in which $\sum_{i\to a} \equiv \sum_i^{occ}\sum_a^{vir}$ and $\sum_{i\to a}\sum_{j\neq i\to a} \equiv \sum_i^{occ}\sum_{j\neq i}^{occ}\sum_a^{vir}$; w_{ia} is coefficient of excited Slater determinant ψ_i^a in an electronically excited electronic state; $\phi_i(\mathbf{r})$ and $\phi_j(\mathbf{r})$ are MOs that hole occupies; $\phi_a(\mathbf{r})$ and $\phi_b(\mathbf{r})$ are MOs that electron occupies. In these equations, the first and second terms stand for contributions of local and cross terms. It is clear that these two electron and hole densities satisfy $\int \rho^{hole}(\mathbf{r})\, d\mathbf{r} = 1$ and $\int \rho^{electron}(\mathbf{r})\, d\mathbf{r} = 1$ due to orthonormality properties of MOs and total sum of squares of all configuration coefficients is 1.0, which means that only one electron is excited leaving one hole. On the basis of electron and hole densities, useful parameters to characterize electron-hole separation can be defined, such as distance of centroids of electron and hole.

Based on density distributions of hole and electron, centroids of hole and electron can be calculated to approximately represent positions of hole and electron. In such case, centroid coordinates X, Y, and Z of electron can be calculated as

$$X_{electron} = \int x\rho^{electron}(\mathbf{r})\, d\mathbf{r} \tag{23}$$

$$Y_{electron} = \int y\rho^{electron}(\mathbf{r})\, d\mathbf{r} \tag{24}$$

$$Z_{electron} = \int z\rho^{electron}(\mathbf{r})\, d\mathbf{r} \tag{25}$$

where x, y, and z are Cartesian coordinate components of electron. Similarly, one can define those for hole. Based on centroids of hole and electron, the electron-hole distance is estimated as

$$\sqrt{(D_x)^2 + (D_y)^2 + (D_z)^2}$$

in which $D_x = \mid X_{ele} - X_{hole} \mid$, $D_y = \mid Y_{ele} - Y_{hole} \mid$, and $D_z = \mid Z_{ele} - Z_{hole} \mid$. This distance, called D index in the main text, can be used to evaluate charge separation process. In the present work, time-dependent D index is calculated on the basis of time-dependent densities of electron and hole.

Additional Figures

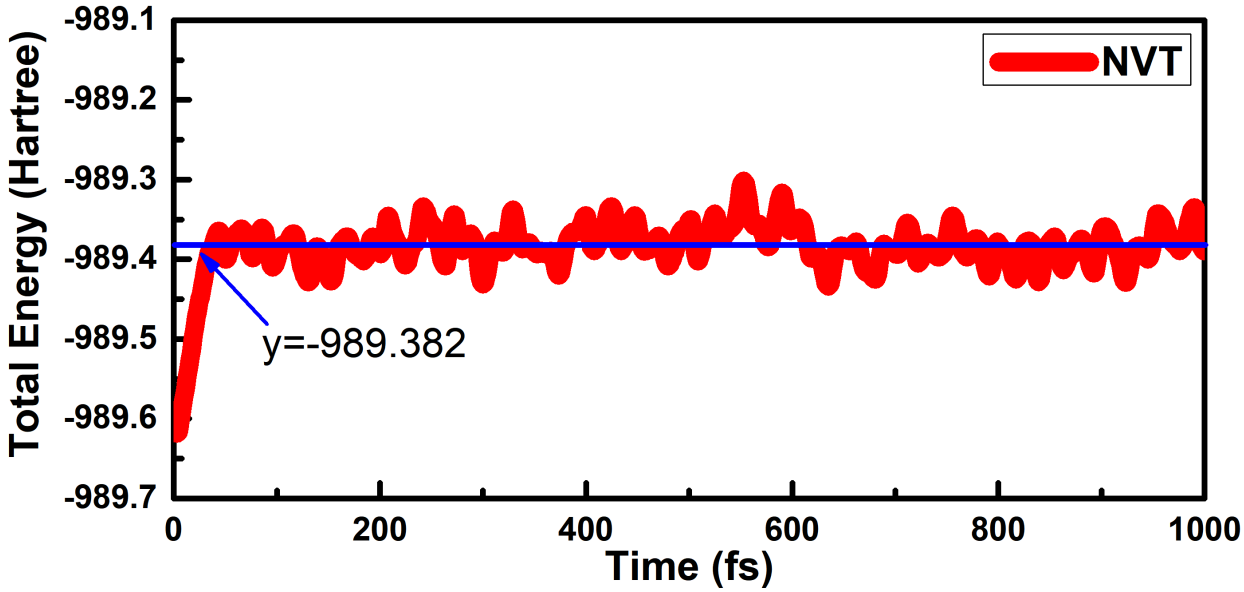

Figure 1: The time-dependent total energies of the PTB7:PDI heterostructure during 1 ps NVT molecular dynamics simulations.

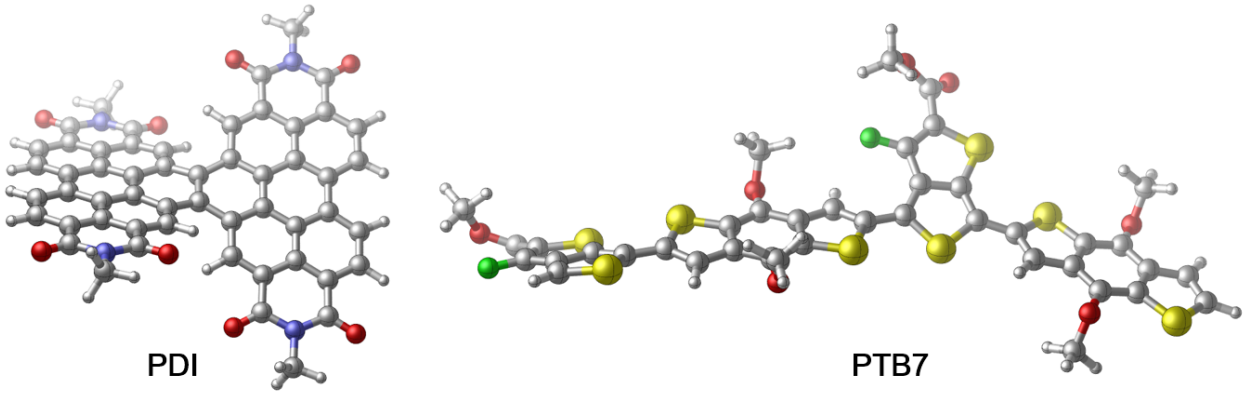

Figure 2: The structures of PDI and PTB7 molecule optimized at B3LYP+D3 level.

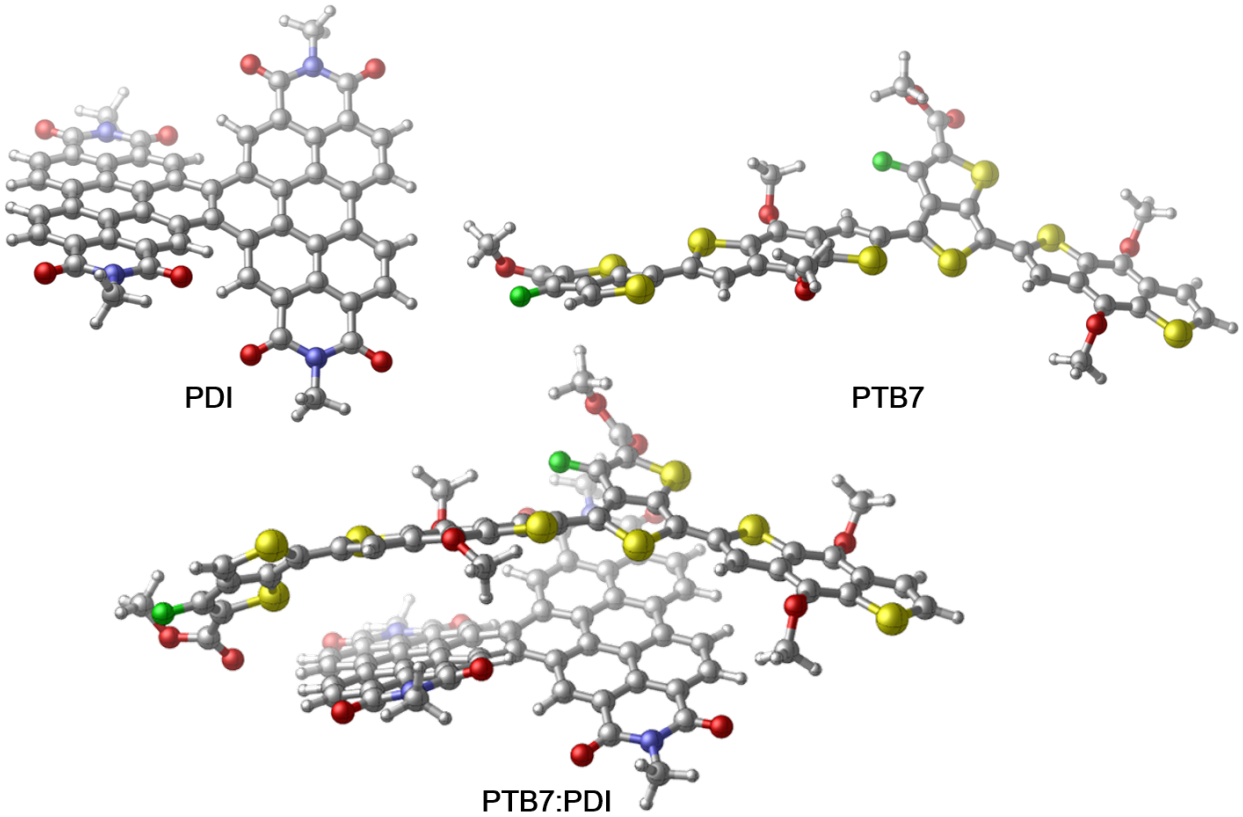

Figure 3: The structures optimized without van der Waals corrections of PDI, PTB7 and PTB7:PDI interface studied in present work.

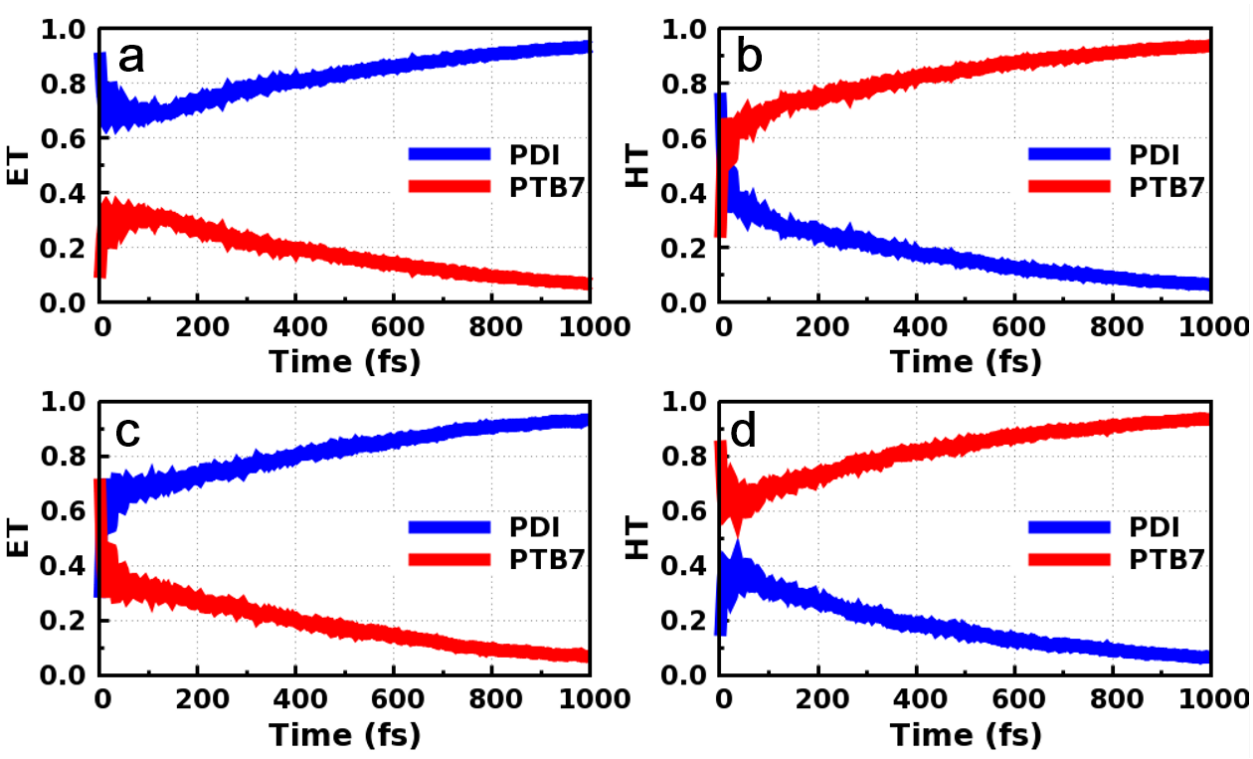

Figure 4: Time-dependent electron and hole transfer dynamics excited PDI (a and b) and PBI (c and d) only respectively.

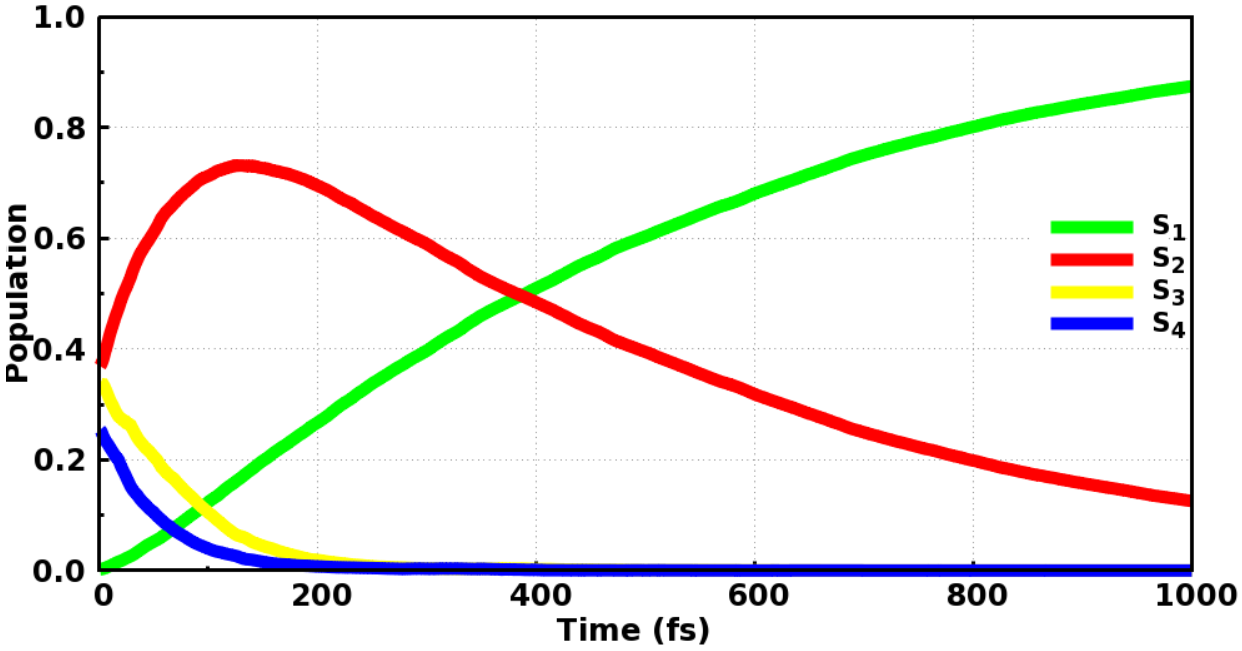

Figure 5: Time-dependent populations of involved excited singlet states of PTB7:PDI interface calculated based on our dynamics simulations.

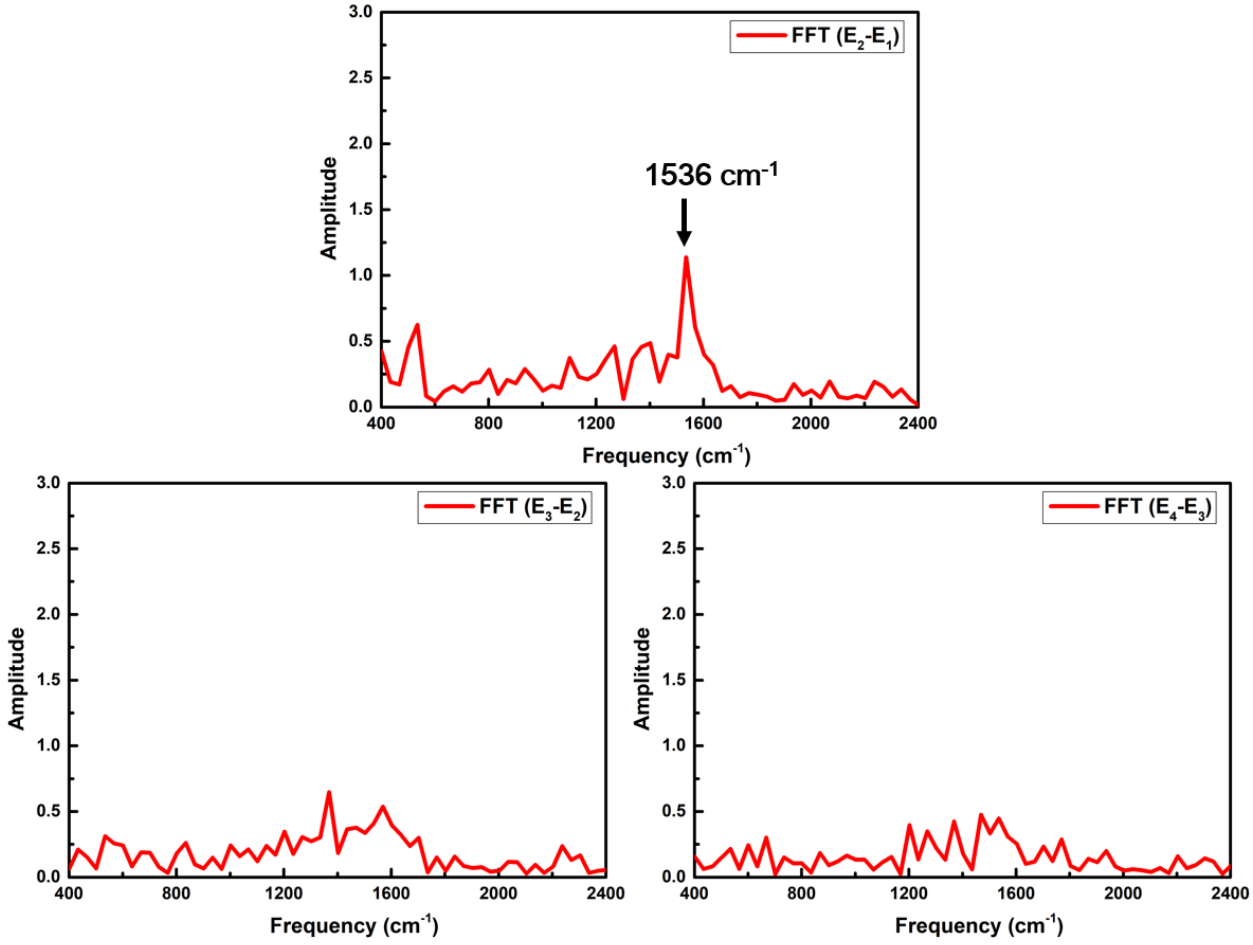

Figure 6: The Fourier transformation of the relevant energy differences of adjacent excited states.

References

(1) Barbatti, M.; Aquino, A. J. A.; Lischka, H. The UV Absorption of Nucleobases: Semi-Classical Ab Initio Spectra Simulations. *Phys. Chem. Chem. Phys.* **2010**, *12*, 4959–4967.

(2) Crespo-Otero, R.; Barbatti, M. Spectrum Simulation and Decomposition with Nuclear Ensemble: Formal Derivation and Application to Benzene, Furan and 2-Phenylfuran. *Theor. Chem. Acc.* **2012**, *131*, 1237.

(3) Liu, X.-Y.; Xie, X.-Y.; Fang, W.-H.; Cui, G. L. Photoinduced Relaxation Dynamics of Nitrogen-Capped Silicon Nanoclusters: a TD-DFT study. *Mol. Phys.* **2018**, *116*, 869–884.

(4) Liu, X.-Y.; Li, Z.-W.; Fang, W.-H.; Cui, G. L. Nonadiabatic Dynamics Simulations on Internal Conversion and Intersystem Crossing Processes in Gold(I) Compounds. *J. Chem. Phys.* **2018**, *149*, 044301.

(5) Liu, X.-Y.; Zhang, Y.-H.; Fang, W.-H.; Cui, G. L. Early-Time Excited-State Relaxation Dynamics of Iridium Compounds: Distinct Roles of Electron and Hole Transfer. *J. Phys. Chem. A* **2018**, *122*, 5518–5532.

(6) Fang, Y.-G.; Peng, L.-Y.; Liu, X.-Y.; Fang, W.-H.; Cui, G. L. QM/MM Nonadiabatic Dynamics Simulation on Ultrafast Excited-State Relaxation in Osmium(II) Compounds in Solution. *Comput. Theor. Chem.* **2019**, *1155*, 90–100.

(7) Tully, J. C.; Preston, R. K. Trajectory Surface Hopping Approach to Nonadiabatic Molecular Collisions: Reaction of H^+ with D2. *J. Chem. Phys.* **1971**, *55*, 562–572.

(8) Hammes-Schiffer, S.; Tully, J. C. Proton Transfer in Solution: Molecular Dynamics with Quantum Transitions. *J. Chem. Phys.* **1994**, *101*, 4657–4667.

(9) Barbatti, M.; Aquino, A. J. A.; Szymczak, J. J.; Nachtigallová, D.; Hobza, P.; Lischka, H. Relaxation Mechanisms of UV-Photoexcited DNA and RNA Nucleobases. *Proc. Natl. Acad. Sci. U. S. A.* **2010**, *107*, 21453–21458.

(10) Lu, Y.; Lan, Z. G.; Thiel, W. Hydrogen Bonding Regulates the Monomeric Nonradiative Decay of Adenine in DNA Strands. *Angew. Chem. Int. Ed.* **2011**, *50*, 6864–6867.

(11) Cui, G. L.; Lan, Z. G.; Thiel, W. Intramolecular Hydrogen Bonding Plays a Crucial Role in the Photophysics and Photochemistry of the GFP Chromophore. *J. Am. Chem. Soc.* **2012**, *134*, 1662–1672.

(12) Long, R.; English, N. J.; Prezhdo, O. V. Photo-Induced Charge Separation across the Graphene-TiO_2 Interface Is Faster Than Energy Losses: A Time-Domain ab Initio Analysis. *J. Am. Chem. Soc.* **2012**, *134*, 14238–14248.

(13) Fazzi, D.; Barbatti, M.; Thiel, W. Unveiling the Role of Hot Charge-Transfer States in Molecular Aggregates via Nonadiabatic Dynamics. *J. Am. Chem. Soc.* **2016**, *138*, 4502–4511.

(14) Fischer, S. A.; Chapman, C. T.; Li, X. S. Surface Hopping with Ehrenfest Excited Potential. *J. Chem. Phys.* **2011**, *135*, 144102.

(15) Fischer, S. A.; Lingerfelt, D. B.; May, J. W.; Li, X. S. Non-Adiabatic Molecular Dynamics Investigation of Photoionization State Formation and Lifetime in Mn^{2+}-Doped ZnO Quantum Dots. *Phys. Chem. Chem. Phys.* **2014**, *16*, 17507–17514.

(16) Nelson, T.; Fernandez-Alberti, S.; Roitberg, A. E.; Tretiak, S. Nonadiabatic Excited-State Molecular Dynamics: Modeling Photophysics in Organic Conjugated Materials. *Acc. Chem. Res.* **2014**, *47*, 1155–1164.

(17) Richter, M.; Marquetand, P.; González-Vázquez, J.; Sola, I.; González, L. SHARC: ab Initio Molecular Dynamics with Surface Hopping in the Adiabatic Representation Including Arbitrary Couplings. *J. Chem. Theory Comput.* **2011**, *7*, 1253–1258.

(18) Richter, M.; Marquetand, P.; González-Vázquez, J.; Sola, I.; González, L. Femtosecond Intersystem Crossing in the DNA Nucleobase Cytosine. *J. Phys. Chem. Lett.* **2012**, *3*, 3090–3095.

(19) Wang, Y.-T.; Liu, X.-Y.; Cui, G. L.; Fang, W.-H.; Thiel, W. Photoisomerization of Arylazopyrazole Photoswitches: Stereospecific Excited-State Relaxation. *Angew. Chem. Int. Ed.* **2016**, *55*, 14009–14013.

(20) Wang, Y.-T.; Gao, Y.-J.; Wang, Q.; Cui, G. L. Photochromic Mechanism of a Bridged Diarylethene: Combined Electronic Structure Calculations and Nonadiabatic Dynamics Simulations. *J. Phys. Chem. A* **2017**, *121*, 793–802.

(21) Xia, S.-H.; Cui, G. L.; Fang, W.-H.; Thiel, W. How Photoisomerization Drives Peptide Folding and Unfolding: Insights from QM/MM and MM Dynamics Simulations. *Angew. Chem. Int. Ed.* **2016**, *55*, 2067–2072.

(22) Xia, S.-H.; Xie, B.-B.; Fang, Q.; Cui, G. L.; Thiel, W. Excited-State Intramolecular Proton Transfer to Carbon Atoms: Nonadiabatic Surface-Hopping Dynamics Simulations. *Phys. Chem. Chem. Phys.* **2015**, *17*, 9687–9697.

(23) Gao, Y.-J.; Chang, X.-P.; Liu, X.-Y.; Li, Q.-S.; Cui, G. L.; Thiel, W. Excited-State Decay Paths in Tetraphenylethene Derivatives. *J. Phys. Chem. A* **2017**, *121*, 2572–2579.

(24) Zhang, Y. H.; Sun, X. W.; Zhang, T. S.; Liu, X. Y.; Cui, G. L. Nonadiabatic Dynamics Simulations on Early-Time Photochemistry of Spirobenzopyran. *J. Phys. Chem. A* **2020**, *124*, 2547–2559.

(25) Cui, G. L.; Thiel, W. Generalized Trajectory Surface-Hopping Method for Internal Conversion and Intersystem Crossing. *J. Chem. Phys.* **2014**, *141*, 124101.

(26) Liu, X.-Y.; Li, Z.-W.; Fang, W.-H.; Cui, G. L. Nonadiabatic Exciton and Charge Separation Dynamics at Interfaces of Zinc Phthalocyanine and Fullerene: Orientation Does Matter. *J. Phys. Chem. A* **2020**, *124*, 7388–7398.

(27) Send, R.; Furche, F. First-Order Nonadiabatic Couplings from Time-Dependent Hybrid Density Functional Response Theory: Consistent Formalism, Implementation, and Performance. *J. Chem. Phys.* **2010**, *132*, 044107.

(28) Li, Z.; Liu, W. First-Order Nonadiabatic Coupling Matrix Elements between Excited States: A Lagrangian Formulation at the CIS, RPA, TD-HF, and TD-DFT Levels. *J. Chem. Phys.* **2014**, *141*, 014110.

(29) Li, Z.; Suo, B.; Liu, W. First Order Nonadiabatic Coupling Matrix Elements between Excited States: Implementation and Application at the TD-DFT and pp-TDA Levels. *J. Chem. Phys.* **2014**, *141*, 244105.

(30) Pittner, J.; Lischka, H.; Barbatti, M. Optimization of Mixed Quantum-Classical Dynamics: Time-Derivative Coupling Terms and Selected Couplings. *Chem. Phys.* **2009**, *356*, 147–152.

(31) Ryabinkin, I. G.; Nagesh, J.; Izmaylov, A. F. Fast Numerical Evaluation of Time-Derivative Nonadiabatic Couplings for Mixed Quantum-Classical Methods. *J. Phys. Chem. Lett.* **2015**, *6*, 4200–4203.

(32) Plasser, F.; Lischka, H. Analysis of Excitonic and Charge Transfer Interactions from Quantum Chemical Calculations. *J. Chem. Theory Comput.* **2012**, *8*, 2777–2789.

(33) Huang, J.; Du, L.; Hu, D.; Lan, Z. G. Theoretical Analysis of Excited States and Energy Transfer Mechanism in Conjugated Dendrimers. *J. Comput. Chem.* **2015**, *36*, 151–163.

(34) Lu, T.; Chen, F. Multiwfn: A Multifunctional Wavefunction Analyzer. *J. Comput. Chem.* **2012**, *33*, 580–592.

(35) Lu, T. Multiwfn Manual, version 3.6(dev), Section 3.21.1, available at http://sobereva.com/multiwfn. 2018.